# Production of the $^1S_0$ diproton in the $pp \to pp\pi^0$ reaction at 0.8 GeV

S. Dymov [a], D. Gusev [a], M. Hartmann [b], V. Hejny [b],
A. Kacharava [c,d], A. Khoukaz [e], V. Komarov [a], P. Kulessa [f],
A. Kulikov [a], V. Kurbatov [a], N. Lang [e], G. Macharashvili [a,d],
T. Mersmann [e], S. Merzliakov [a,b], S. Mikirtytchiants [g],
A. Mussgiller [b], D. Prasuhn [b], F. Rathmann [b], R. Schleichert [b],
H. Ströher [b], Yu. Uzikov [a], C. Wilkin [h], and S. Yaschenko [c,a].

[a]*Laboratory of Nuclear Problems, Joint Institute for Nuclear Research, 141980 Dubna, Russia*

[b]*Institut für Kernphysik, Forschungszentrum Jülich, 52425 Jülich, Germany*

[c]*Physikalisches Institut II, Universität Erlangen–Nürnberg, 91058 Erlangen, Germany*

[d]*High Energy Physics Institute, Tbilisi State University, 0186 Tbilisi, Georgia*

[e]*Institut für Kernphysik, Universität Münster, 48149 Münster, Germany*

[f]*Institute of Nuclear Physics, 31342 Cracow, Poland*

[g]*St. Petersburg Nuclear Physics Institute, 188350 Gatchina, Russia*

[h]*Physics and Astronomy Department, UCL, London, WC1E 6BT, UK*

## Abstract

The $pp \to pp\pi^0$ differential cross section has been measured with the ANKE spectrometer at COSY–Jülich for pion cms angles between 0° and 15.4° at a proton beam energy of 0.8 GeV. The selection of diproton pairs with an excitation energy $E_{pp} < 3$ MeV ensures that the final $pp$ system is dominantly in the spin–singlet $^1S_0$ state. The kinematics are therefore very similar to those of $pp \to d\pi^+$ but with different spin and isospin transitions. The results will thus provide a crucial extra test of pion production models in nucleon–nucleon collisions.

The cross sections, which are over two orders of magnitude smaller than those of $pp \to d\pi^+$, show a forward dip, even stronger than that seen at lower energies. This behaviour is well reproduced in a theoretical model that includes $P$–wave $\Delta N$ states.

arXiv:nucl-ex/0512035v1  22 Dec 2005

Single pion production in nucleon–nucleon collisions, $NN \rightarrow NN\pi$, is the first inelastic process that can be used to test our understanding of the underlying meson–baryon dynamics of the $NN$ interaction [1,2,3]. By far the cleanest reaction to study is $pp \rightarrow d\pi^+$, where the differential cross section and multitude of spin observables that have been measured over the years [4] can confront the different theoretical models.

In contrast, very little was known about the $pp \rightarrow pp\pi^0$ reaction, though the unexpectedly large $\pi^0$ production rate observed near threshold [5] led to a flurry of theoretical activity [6]. Now in cases where the excitation energy $E_{pp}$ of the final protons is very small, due to the Pauli principle, this reaction will excite only the $J^p = 0^+$ ($^1S_0$) diproton state. Despite having kinematics very similar to those of $pp \rightarrow d\pi^+$, this reaction involves different transitions in the $NN$ system and, in particular, the role of the $\Delta$ isobar is expected to be much suppressed because the $S$–wave $\Delta N$ intermediate state is forbidden.

Some information on the transitions involved has been extracted from quasi–free pion absorption on $^3$He [7]. However, previous measurements of the differential cross sections for $pp \rightarrow \{pp\}_s\pi^0$ have only been carried out up to a beam energy of 425 MeV, with a cut imposed on the excitation energy of $E_{pp} < 3$ MeV [8,9]. This value satisfies the requirement that the spin–singlet $S$-wave ($^1S_0$) final state, here denoted by $\{pp\}_s$, should dominate while providing reasonable statistics. One important feature of the experimental data is that with the $E_{pp}$ selection the cross sections show a forward dip whereas, if no cut is applied on the excitation energy, then for the higher beam energies there is a forward maximum [9,10].

Now 425 MeV is below the threshold of $N\Delta$ production; the data show no sign of being influenced in any clear way by the $\Delta$ and we need to go to higher energy to investigate the effects of $P$–wave $\Delta N$ systems. As part of a programme to investigate the small $E_{pp}$ region in intermediate energy nuclear reactions, in particular in large momentum transfer deuteron breakup reactions [11,12], we have carried out a high statistics measurement of the $pp \rightarrow \{pp\}_s\pi^0$ reaction at $T_p = 800$ MeV for pion cm angles below 15.4°.

The experiment was performed at the magnetic spectrometer ANKE [13], placed at an internal target position of the COSY COoler SYnchrotron [14]. Fast charged particles, resulting from the interaction of the proton beam with the hydrogen cluster–jet target [15], were registered in the Forward Detector (FD) system [16]. Its hodoscope provided a trigger signal and an energy–loss measurement. It also allowed a determination of the differences in arrival times for particle pairs hitting different counter elements. The tracking system gave a momentum resolution $\sigma_p/p \approx 0.8 - 1.2\%$ for protons in the range $(0.5 - 1.2)$ GeV/c.
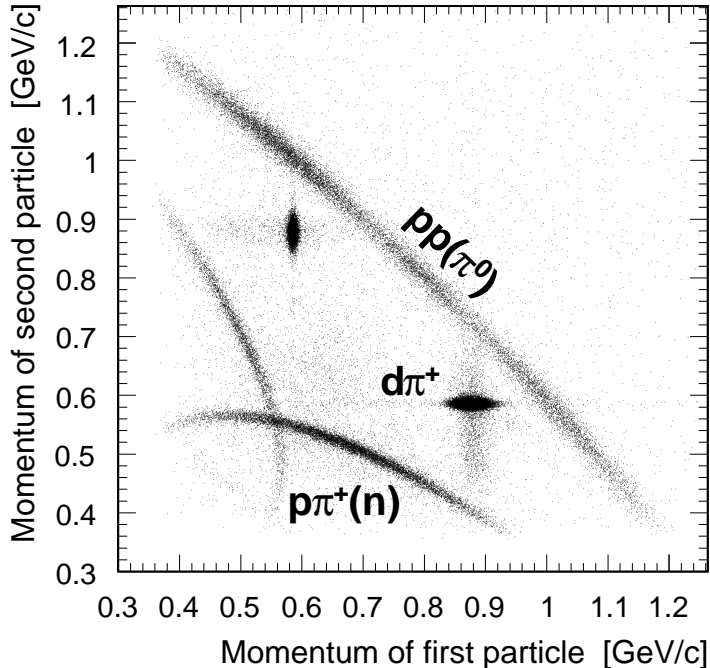
Fig. 1. Scatter plot of the magnitudes of the momenta of two charged particles detected in the FD. The selection procedure introduces a slight bias as to which particle is called "1", but this does not affect the subsequent analysis.

The trigger used required the crossing of the two planes of the scintillation hodoscopes by at least one charged particle but, in the subsequent off–line analysis of the $pp \to \{pp\}_s \pi^0$ reaction, only events with two tracks in the FD were retained. In Fig. 1 is shown a two–dimensional scatter plot of the magnitudes of their two momenta corresponding to about half of our statistics. Due to the limited angular acceptance of ANKE, there are kinematic correlations for reactions with two and three particle in the final state. One therefore sees in the figure islands corresponding to $pp \to d\pi^+$ and bands resulting from $pp \to pn\pi^+$ and $pp \to pp\pi^0$. Candidates for the latter reaction are well separated from the other processes. Furthermore, in approximately 75% of cases the particles hit different counters in the hodoscope and the difference in their arrival time could also be used in the selection. The $d\pi^+$ pairs coming from the $pp \to d\pi^+$ reaction, which could potentially provide the most serious physical background, are separated from the $pp$ pairs from $pp \to pp\pi^0$ in time difference by more than at 8 ns, whereas the actual resolution is better than 0.5 ns

The distributions of missing mass squared, $M_X^2$, are shown separately in Fig. 2 for single–counter and double–counter candidates with low excitation energy in the $pp$ system, $E_{pp} < 3$MeV. In both cases one sees a very clean $\pi^0$ peak centred at 0.021 $(\text{GeV}/\text{c}^2)^2$, which agrees with $m_{\pi^0}^2$ to well within our experimental precision. The widths of the Gaussian fits are compatible with those obtained from Monte Carlo simulations; the marginally narrower peak in the single–
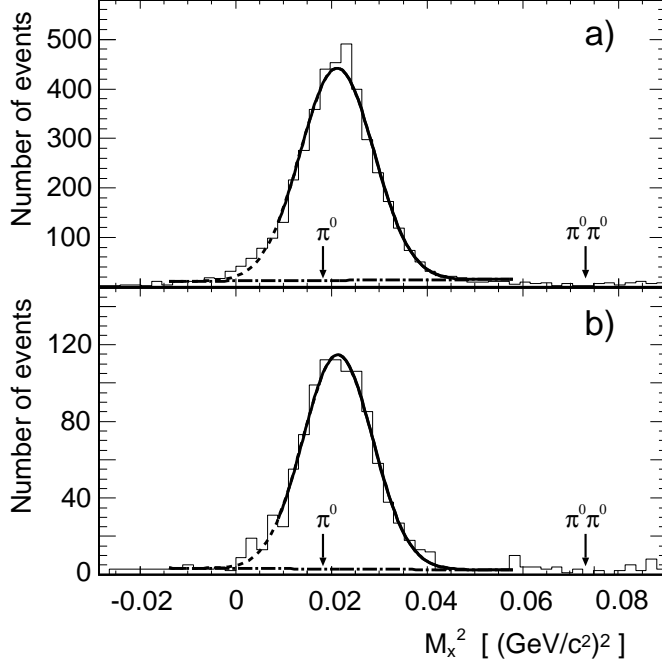
3

Fig. 2. Distributions in the square of the missing mass for candidates for the $pp \to ppX$ reaction with excitation energy $E_{pp} < 3$ MeV and $\theta_{pp}^{cm} \leq 15.4°$ when the protons (a) hit different counters, and (b) the same counter. From the indicated positions of the $\pi^0$ peak and the $2\pi^0$ threshold it is seen that single and double pion production can be clearly separated. Gaussian fits to the $\pi^0$ peak plus a constant background yield a total number of $\pi^0$ events in (a) and (b) of respectively 4425 and 1008.

counter data is due to these events generally having a smaller opening angle resulting in the kinematics being slightly better defined. The backgrounds are small and slowly varying and two–pion production can be clearly excluded in either case. There is a small excess of events observed on the left side of the $\pi^0$ peak. These may correspond to single photon production through $pp \to \{pp\}_s \gamma$ and so the regions indicated by dashed lines in Fig. 2 have not been included in the Gaussian fits. Since this interpretation is not unambiguous and these events might still correspond to good $\pi^0$ events, we have added an extra 2% to the systematic error. Given that the two data sets are completely compatible, they have been grouped together in the subsequent analysis. The resolution in excitation energy for the combined $pp \to pp\pi^0$ events was $\sigma(E_{pp}) \approx 0.2$–0.3 MeV for $E_{pp}$ in the range 0–3 MeV.

The value of the luminosity needed to determine the cross section was found by comparing the yield of $pp$ elastic scattering, measured simultaneously with the other reactions, with that deduced from the SAID data base [17]. The integrated luminosity obtained from this is $L_{int} = (6.72 \pm 0.26) \times 10^{34}$ cm$^{-2}$, where the error comes mainly from averaging over the angular bins.

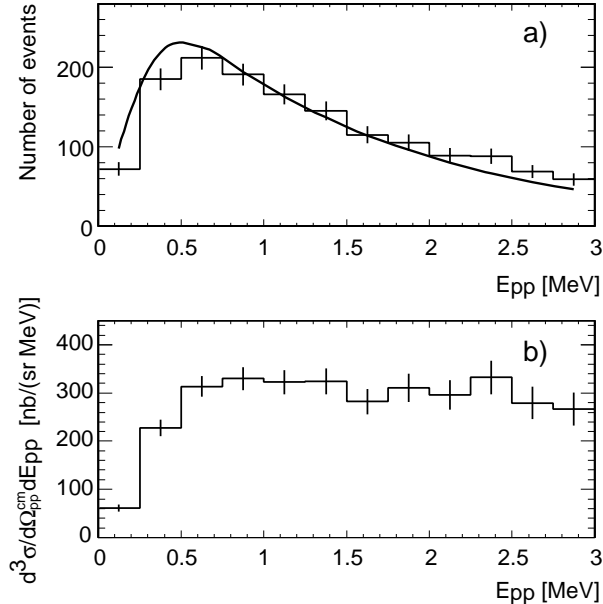In order to determine the triply differential cross section $\mathrm{d}^3\sigma/(\mathrm{d}\Omega_{pp}^{cm}\,\mathrm{d}E_{pp})$,

4

Fig. 3. (a) Number of $pp \to pp\pi^0$ events in the interval $8.9° < \theta_{pp}^{cm} < 13°$ as a function of $E_{pp}$; (b) The same data corrected for acceptance and detection efficiency and presented as differential cross sections. Only statistical errors are shown. The curve results from passing the Migdal–Watson function $|T(E_{pp})|^2$ of Eq. (1), multiplied by phase space, through a Monte Carlo simulation of the ANKE apparatus and normalising the predictions to the summed experimental histogram. Similar results are found for the other angular intervals.

events selected in the range $0 \leq E_{pp} < 3$ MeV were divided into groups of equal intervals in $\cos\theta_{pp}^{cm}$. The energy spectrum of counts in the angular interval $8.9° < \theta_{pp}^{cm} < 13°$ is shown in Fig. 3a. The spectra in the other intervals demonstrate a similar behaviour. Values of the corresponding cross sections were obtained from such a distribution by taking into account geometrical acceptance, efficiency in the track recognition algorithm for two particles, interactions in the constituent materials, efficiency and resolution of the detectors and other known effects on the basis of a Monte Carlo simulation of the ANKE setup. This leads to the histogram with the statistical errors presented in Fig. 3b.

The rapid rise of the spectrum with $E_{pp}$ from threshold illustrated in Fig. 3b is typical of all intermediate energy reactions where one produces proton pairs and is induced by the $pp$ final state interaction. We have indeed observed exactly the same phenomenon in the $pd \to (pp)n$ reaction with the same apparatus at ANKE [11,12]. This effect is often parameterised, in the Migdal–Watson approximation [18], by the square of the low energy $pp$ elastic scattering amplitude for which

$$|T(E_{pp})|^2 = \frac{1}{|C(\eta)|^2} \left(\frac{\sin\delta}{k}\right)^2, \tag{1}$$

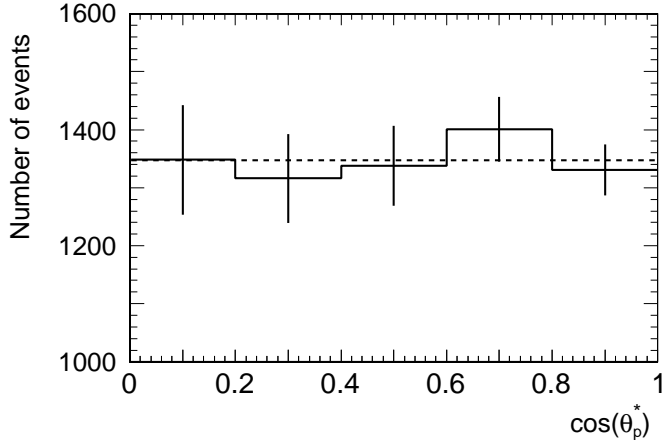where $|C(\eta)|^2$ is the Coulomb penetration factor evaluated at $\eta = \alpha m_p/2k =$

Fig. 4. Distribution of acceptance–corrected $pp \to \{pp\}_s \pi^0$ events with $E_{pp} < 3\mathrm{MeV}$ over $\cos\theta_p^*$, where $\theta_p^*$ is the angle between the directions of the proton and diproton momenta in the centre of mass of the diproton. Note that the vertical scale does not start from zero.

$\alpha\sqrt{m_p/E_{pp}}/2$, and $\delta$ is the combined Coulomb–nuclear phase shift. This has been evaluated numerically for the Reid soft core potential, for which the scattering length $a_{pp} = -7.8\,\mathrm{fm}$.

The Migdal–Watson factor of Eq. (1) was used as an event generator together with phase space to provide candidates which were then traced through the experimental setup, taking into account all its known features. The resulting smoothed curve, shown in Fig. 3a, provides a semi–quantitative description of the data which is quite sufficient for our purpose, where we quote cross sections summed over energy. The data are a little above the curves at the higher $E_{pp}$ and we cannot exclude some small $P$–wave contribution though globally the angular distribution of the $pp$ system in its rest frame shown in Fig. 4 is consistent with isotropy. It should be noted that the $^1P_0$ final state would also produce a flat distribution.

Due to the identity of the initial protons, the differential cross section is an even function of $\cos\theta_\pi^{cm}$ and in Fig. 5 it is plotted *versus* $\cos^2\theta_\pi^{cm}$. The results show a monotonic decrease towards the forward direction and, as seen from the figure, they can be well parameterised by the linear function $a(1 + b\sin^2\theta_\pi^{cm})$, where $a = (704 \pm 22_{\mathrm{stat}} \pm 32_{\mathrm{syst}})$ nb/sr and $b = 5.6 \pm 1.2$. With the same $E_{pp}$ cut as used here, a similar forward dip was observed in this reaction at lower energies, $T_p \leq 425$ MeV [8,9], though for these energies it was found that $b$ was much smaller, being always less than 1.4. Since, for such small values of $E_{pp}$, the final diproton must be dominantly in an $S$–wave, constraints from spin–parity and Fermi statistics then require the pion to be in an even partial wave. As a consequence, the forward dip was attributed to an interference between the pion $s$ and $d$ waves [9]. Given that the influence of $d$–waves might be expected to increase with energy, it is perhaps not surprising that we find
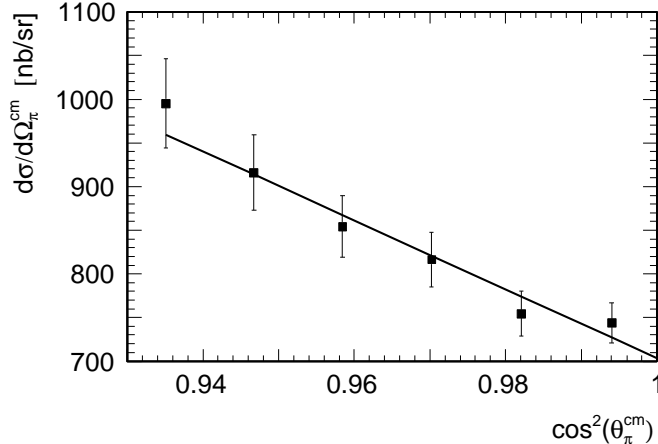
6

Fig. 5. The measured $pp \to \{pp\}_s \pi^0$ differential cross section for $E_{pp} < 3$ MeV as a function of $\cos^2(\theta_\pi^{cm})$. The curve is a straight–line fit to the data.

a larger slope parameter at 800 MeV.

Preliminary theoretical predictions have been made for the $pp \to \{pp\}_s \pi^0$ differential cross section at 800 MeV in a model that includes contributions from $P$–wave $\Delta N$ intermediate states [19,20]. The overall magnitude is similar to that which we have observed and, in particular, the forward slope, driven by the pion $d$–wave, is well reproduced. It is expected that our data, combined with those at lower energies, will allow such models to be refined.

Though we have argued that the kinematics of $pp \to \{pp\}_s \pi^0$ and $pp \to d\,\pi^+$ are quite similar, the underlying dynamics must be very different. This is illustrated in Table 1, where we show the values of the two differential cross sections and their ratio $R(\pi^0/\pi^+)$ in the forward direction obtained at different energies. The results seem to indicate that there might be a broad minimum in $R$ in the $\Delta$ region of the $pp \to d\pi^+$ reaction.

The GEM collaboration has recently published high precision data on the ratio of the forward production of pions in the $pp \to \pi^+ d$ and $pp \to \pi^+ pn$ reactions at 981 MeV [21]. Since the spin–singlet $pn$ final state interaction has a much sharper energy dependence than that of the triplet, from the shape of the pion momentum spectrum they could put an upper limit on the amount of $pn$ singlet produced. Integrating over excitation energies $E_{pn} <$ 3 MeV, it is seen that the ratio of $\dfrac{d\sigma}{d\Omega}(pp \to \{pn\}_s \pi^+)$ to $\dfrac{d\sigma}{d\Omega}(pp \to d\pi^+)$ could be at most about 5%. If Coulomb effects are ignored, the cross sections for spin–singlet production through $pp \to \{pn\}_s \pi^+$ and $pp \to \{pp\}_s \pi^0$ should be identical. Though Coulomb suppression in the $\{pp\}_s$ final state will be large, it looks very doubtful whether the study of the spectrum alone will be sufficient to isolate the $pp \to \{pn\}_s \pi^+$ cross section in view of the values presented in Table 1. Measuring the proton and pion in coincidence, as has been done for

7

| $T_p$ | $\sigma(pp\pi^0)$ | $\sigma(d\pi^+)$ | $R(\pi^0/\pi^+)$ |
|---|---|---|---|
| (MeV) | (nb/sr) | ($\mu$b/sr) | $\times 10^3$ |
| 310 | $109 \pm 8$ | $14.1 \pm 0.3$ | $7.7 \pm 0.6$ |
| 320 | $110 \pm 6$ | $22.1 \pm 0.6$ | $5.0 \pm 0.3$ |
| 340 | $95 \pm 10$ | $41.9 \pm 1.5$ | $2.3 \pm 0.3$ |
| 360 | $86 \pm 7$ | $67.1 \pm 2.7$ | $1.3 \pm 0.1$ |
| 400 | $121 \pm 9$ | $135 \pm 2$ | $0.9 \pm 0.1$ |
| 425 | $171 \pm 14$ | $189 \pm 3$ | $0.9 \pm 0.1$ |
| 800 | $704 \pm 22$ | $155 \pm 4$ | $4.5 \pm 0.4$ |

Table 1
Zero degree differential cross sections for $pp \to \{pp\}_s \pi^0$ with $E_{pp} < 3$ MeV from the present experiment at 800 MeV with the lower energy data being taken from Ref. [9]. The values of the $pp \to d\pi^+$ cross sections are obtained from the SAID SP96 solution with the range of the other solutions being taken as a rough estimate of the error bars [17]. The ratio $R(\pi^0/\pi^+)$ of the two pion–production cross sections is also presented.

example in Refs. [22,23] and analysed in a model–independent way [24], still only provides upper bounds. The study of $\pi^0$ production therefore seems to be the most realistic way of investigating the ${}^1S_0$ final state here.

Data on quasi–free pion production in the $pd \to \{pp\}_s X$ reaction were obtained as a by–product of our deuteron break-up measurements [11] and these results will be interpreted in terms of the sum of the cross sections for $pp \to \{pp\}_s \pi^0$ and $pn \to \{pp\}_s \pi^-$. At 800 MeV it will then be possible to subtract the $\pi^0$ contribution reported here in order to obtain data on $\pi^-$ production.

It is intriguing to note that a very similar ratio to that of Table 1 has been observed for backward dinucleon production in the $pd \to \{pp\}_s n$ and $pd \to dp$ reactions at intermediate energies [11]. Now such a connection would be natural within a one–pion–exchange mechanism, where the large momentum transfer $pd \to dp$ reaction is driven by a $pp \to d\pi^+$ sub-process [25,26]. More quantitative estimates of the $pd \to \{pp\}_s n$ cross section, where the $pp \to \{pp\}_s \pi^0$ sub-process is used rather than the $pp \to d\pi^+$, are currently under way [27].

It is seen from Table 1 that there is a real lack of data on the $pp \to \{pp\}_s \pi^0$ reaction in the $\Delta$ region and this could be usefully filled by further experiments at ANKE. It should also be noted that, unlike the complicated spin structure connected with the $pp \to d\pi^+$ reaction, only two spin amplitudes which are functions of $\cos^2 \theta_\pi$ are required to describe the $pp \to \{pp\}_s \pi^0$ reaction.

These can be isolated, up to an unmeasurable overall phase, by determining the proton analysing power and the initial $pp$ spin correlation $C_{xx}$. Both of these experiments can be carried out at small angles using ANKE [28] and the resulting amplitude analysis will tie down even further $\pi NN$ dynamics at intermediate energies.

# References

[1]  H. Garcilazo and T. Mizutani, $\pi NN$ *systems* (Singapore, World Scientific, 1990).

[2]  H. Machner and J. Haidenbauer, J. Phys. G **25** (1999) R231.

[3]  C. Hanhart, Phys. Rep. **397** (2004) 155.

[4]  R.A. Arndt et al., Phys. Rev. C **48** (1993) 1926.

[5]  H.O. Meyer et al., Nucl. Phys. A **539** (1992) 633.

[6]  See for example: T.-S.H. Lee and D.O. Riska, Phys. Rev. Lett. **70** (1993) 2237.

[7]  M.A. Moinester et al., Phys. Rev. Lett. **52** (1984) 1203.

[8]  Y. Maeda, N. Matsuoka, and K. Tamura, Nucl. Phys. A **684** (2001) 392c.

[9]  R. Bilger et al., Nucl. Phys. A **693** (2001) 633.

[10] G. Rappenecker et al., Nucl. Phys. A **590** (1995) 763.

[11] V. Komarov et al., Phys. Lett. B **553** (2003) 179.

[12] S. Yaschenko et al., Phys. Rev. Lett. **94** (2005) 072304.

[13] S. Barsov et al., Nucl. Instr. and Meth. A **462** (1997) 364.

[14] R. Maier, Nucl. Instr. and Meth. A **390** (1997) 1.

[15] A. Khoukaz et al., Eur. Phys. J. D **5** (1999) 275.

[16] S. Dymov et al., Part. and Nucl. Lett. **1** No. 2[119] (2004) 40.

[17] SAID data base available from http://gwdac.phys.gwu.edu

[18] K.M. Watson, Phys. Rev. **88** (1952) 1163; A.B. Migdal, Sov. Phys. JETP **1** (1955) 2.

[19] J.A. Niskanen, Phys. Rev. C **43** (1991) 36.

[20] J.A. Niskanen (*in preparation*).

[21] M. Abdel-Bary et al., Phys. Lett. B **610** (2005) 31.

[22] J. Hudomalj-Gabitzsch et al., Phys. Rev. C **18** (1978) 2666.

[23] V. Abaev et al., Phys. Lett. B **521** (2001) 158.

[24] Yu.N. Uzikov and C. Wilkin, Phys. Lett. B **511** (2001) 191.

[25] N.S. Craigie and C. Wilkin, Nucl. Phys. B **14** (1969) 477.

[26] V.M. Kolybasov and N.Ya. Smorodynskaya, Yad. Fiz. **17** (1973) 1211.

[27] Yu.N. Uzikov and C. Wilkin (*in preparation*).

[28] A. Kacharava, F. Rathmann, and C. Wilkin, *Spin Physics from COSY to FAIR*, COSY proposal # 152 (2005) [arXiv:nucl-ex/0511028].